AIP | The Journal of Chemical Physics

Crossed beam investigations of the reaction dynamics of O (3 P) with allyl radical, C 3 H 5

Han-Cheol Kwon, Jong-Ho Park, Hohjai Lee, Hee-Kyung Kim, Young-Sang Choi, and Jong-Ho Choi

Citation: The Journal of Chemical Physics **116**, 2675 (2002); doi: 10.1063/1.1449872
View online: http://dx.doi.org/10.1063/1.1449872
View Table of Contents: http://scitation.aip.org/content/aip/journal/jcp/116/7?ver=pdfcov
Published by the AIP Publishing

JOURNAL OF CHEMICAL PHYSICS VOLUME 116, NUMBER 7 15 FEBRUARY 2002

COMMUNICATIONS

Crossed beam investigations of the reaction dynamics of O(^3P) with allyl radical, C_3H_5

Han-Cheol Kwon, Jong-Ho Park, Hohjai Lee, Hee-Kyung Kim, Young-Sang Choi,
and Jong-Ho Choi[a)]
Department of Chemistry and Center for Electro- and Photo-Responsive Molecules, Korea University, 1, Anam-dong, Seoul 136-701, Korea

(Received 9 July 2001; accepted 18 December 2001)

The reaction of ground-state atomic oxygen (O(^3P)) with allyl radical (C_3H_5) was investigated in the crossed beam configuration. O(^3P) and C_3H_5 were generated by the photodissociation of NO_2 and the supersonic flash pyrolysis of allyl iodide, respectively. The nascent internal distributions of the OH($X^2\Pi : v''=0,1$) reaction product from the newly observed channel of $O(^3P)+C_3H_5 \rightarrow C_3H_4+OH$ were probed by laser induced fluorescence (LIF) spectroscopy. The distributions showed significant excitations with an unusual bimodal feature: the low and high rotational components without spin-orbit and Λ-doublet propensities in the ground and first excited vibrational states. On the basis of population analysis and comparison with the *ab initio* and statistical calculations, the experimental distributions are estimated to be totally non-statistical and suggest that the dynamics of the reaction might be described by two competing mechanisms: a major direct abstraction process and an indirect short-lived addition-complex forming process. © *2002 American Institute of Physics.* [DOI: 10.1063/1.1449872]

INTRODUCTION

Reactions of atomic oxygen with hydrocarbon radicals play an important role in understanding organic synthesis, combustion, and atmospheric and interstellar chemistry. Despite its mechanistic significance, however, difficulties in generating clean and efficient hydrocarbon radicals have resulted in a dearth of information on the reaction dynamics of atom-radicals. In conventional pyrolytic effusion sources, radical species spend a long residence time inside a hot tube, which inevitably leads to radical-radical recombination and/or secondary dissociation. In the supersonic flash pyrolysis source,[1] however, labile organic precursors entrained in a molecular beam undergo a short residence time inside a hot SiC tube and are cleanly pyrolyzed to generate jet-cooled radical beams.

In this communication, we describe our recent investigations of the reaction dynamics of ground-state atomic oxygen (O(^3P)) with allyl radical (C_3H_5). Since allyl is the smallest π-conjugated system stabilized by two resonance structures, and reactive intermediates in many important synthetic reactions, it has long attracted much photochemical and theoretical attention.[2–5]

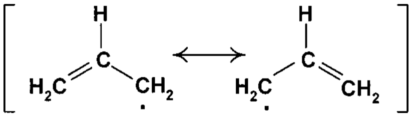

The studies of the reaction dynamics between atomic oxygen and allyl, therefore, provide important insights into atom-radical reactions at the molecular level. While the only channel observed in the previous gas-phase kinetic experiments was the exothermic acrolein channel[6]

$$C_3H_5+O(^3P)\rightarrow C_3H_4O+H \quad \Delta H_f=-63.9\ \text{kcal/mol}, \tag{1}$$

in our crossed beam experiments, however, a second new exothermic channel

$$C_3H_5+O(^3P)\rightarrow C_3H_4+OH \quad \Delta H_f=-45.1\ \text{kcal/mol} \tag{2}$$

was detected by LIF spectroscopy and the nascent internal distributions of the OH product were examined. In addition, we have also performed *ab initio* calculations and prior and RRKM (Rice–Ramsperger–Kassel–Marcus) statistical estimations to facilitate the understanding of the reaction mechanism and dynamic character.[7,8]

EXPERIMENT AND *AB INITIO* CALCULATIONS

Our crossed molecular beam apparatus designed for investigations of reactive scattering will be described in detail elsewhere,[9] and here only a brief relevant account is presented. The apparatus consisting of two source chambers and a scattering chamber was pumped by two 6-in. and one 10-in. baffled diffusion pumps, respectively, and the average base pressure was maintained below 2×10^{-6} Torr.

For the generation of O(^3P), NO_2, seeded in ultra high purity helium (UHP He: 99.999%) at 2 atm stagnation pressure, expanded through a piezoelectrically actuated pulsed nozzle (1.0 mm diam) and was irradiated by ~30 mJ pulses

---

[a)] Author to whom correspondence should be addressed. Telephone: +82-2-3290-3135. Fax: +82-2-3290-3121. Electronic mail: jhc@korea.ac.kr of the 355 nm output (6 mm diam) of the Nd:YAG laser (Continuum Surelite II-10).[10] The allyl radical was produced through a supersonic flash pyrolysis source using the precursor allyl iodide. The precursor, seeded in UHP He at 2 atm, expanded through a pulsed valve (0.8 mm diam, General Valve Co.) with a SiC tube nozzle (1.0 mm diam, 25 mm long, Carborundum Co.). As the gas flew through the SiC channel with a resistively heated length of 10 mm, the precursor was completely pyrolyzed into allyl and atomic iodine, which was confirmed by the saturation of two-photon iodine LIF signals.[4,9] The two reactant beams expanded supersonically into the scattering chamber and were crossed at the center of the chamber.

The OH reaction product was examined by the LIF scheme using the $A\,^2\Sigma^+ - X^2\Pi$ transition in the 306–319 nm region. The output of the Nd:YAG laser-pumped dye laser system (Continuum Surelite III-10, Lambda Physik Scanmate 2) operating on DCM was frequency-doubled in a BBO crystal mounted on an autotracker. The probe laser intensity was carefully controlled such that the excitation was slightly saturated using 3-mm-diam beams over 200 μJ/pulse[10] and the resulting fluorescence signal collected by the PMT (Hamamatsu R212UH) was sent to a boxcar averager (Stanford SR250) interfaced to an IBM PC for display and analysis. The minor interfering background OH signal resulting from the photolysis of impurity HONO always present in the NO_2 beam was subtracted to obtain the OH signal due solely to the reaction.[11,12] No metastable state of atomic oxygen (^1D) has been observed through investigating the reaction of $O(^3P)$ with H_2. The metastable might, if it exists, generate the OH signal due to the large reaction cross-section and exothermicity.

Ab initio calculations of the optimized geometries of the various local minima and transition states were performed at the hybrid density functional B3LYP level using the 6-311G(d,p) basis set.[13–15] Vibrational frequencies were also computed to characterize the stationary points and the zero-point energy corrections (scaling factor of 0.98). All transition structures were confirmed by the single imaginary frequency and the intrinsic reaction coordinate calculations. In addition, the recently developed complete basis set models of CBS-Q and CBS-QB3[16] were used for more accurate and reliable calculations. The calculated reaction enthalpies and heats of formation for various species demonstrated strong agreement with the known experimental values within an accuracy of less than 2 kcal/mol. All calculations were done using the GAUSSIAN 98 system of programs[17] on a IBM PC and a Compaq Workstation (XP-1000).

EXPERIMENTAL RESULTS

A typical LIF spectrum of the $OH(X\,^2\Pi : v''=0,1)$ product obtained from reaction 2 is shown in Fig. 1 and it clearly demonstrated that the nascent OH product exhibits considerable internal excitations. The population analyses for the two spin-orbit states, $F_1(^2\Pi_{3/2})$ and $F_2(^2\Pi_{1/2})$, display bimodal features in both $v''=0$ and 1 vibrational states: the low- and high-N'' rotational components (Fig. 2). For the $v''=0$ level the rotational temperatures are estimated to be 1040 K (F_1) and 970 K (F_2) for the low-N'' component, and 3580 K (F_1) and 3380 K (F_2) for the high-N'' component, assuming Boltzmann distributions. On the other hand, for the $v''=1$ state, while the rotational temperatures for the low-N'' component are found to be 1160 K (F_1) and 1270 K (F_2), the significant temperatures for high-N'' component are not obtained due to the limited number of populations in the distributions.

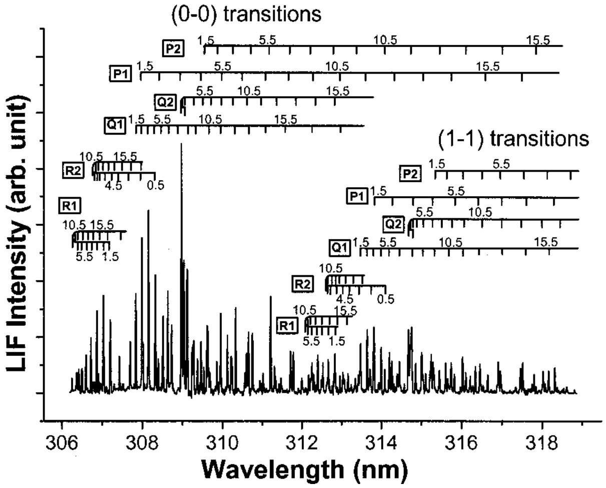

FIG. 1. Experimental $OH(A\,^2\Sigma^+ - X\,^2\Pi)$ LIF spectrum obtained in the reaction of $O(^3P)$ with C_3H_5.

To obtain the ratio of vibrational partitioning (P_1/P_0) for the low- and high-N'' components in the nascent OH states, all of the corresponding rotational populations for the individual branches of $v''=0$ and 1 were summed up, corrected and then compared. The corrections considered in the analysis were the Franck–Condon factors (0.90 and 0.71 for the (0,0) and (1,1) bands, respectively) and the lifetime dif-

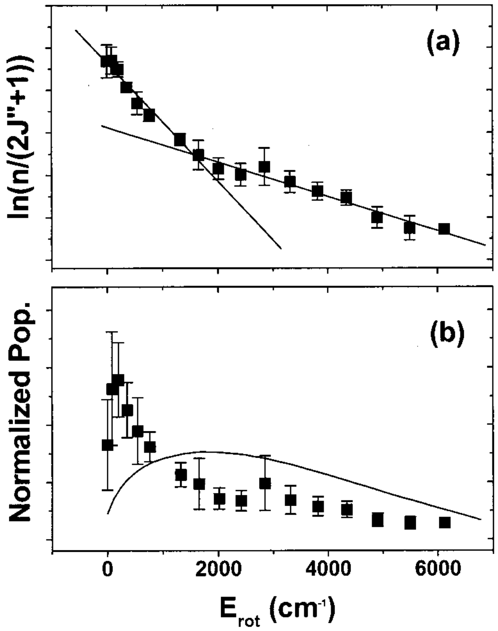

FIG. 2. (a) Nascent rotational population (■) for $v''=0$ (F_1) of OH produced in the reaction of $O(^3P)$ with C_3H_5 with Boltzmann plots for low- and high-N'' components (—) and (b) normalized rotational population (■) with statistical prior plot (—).

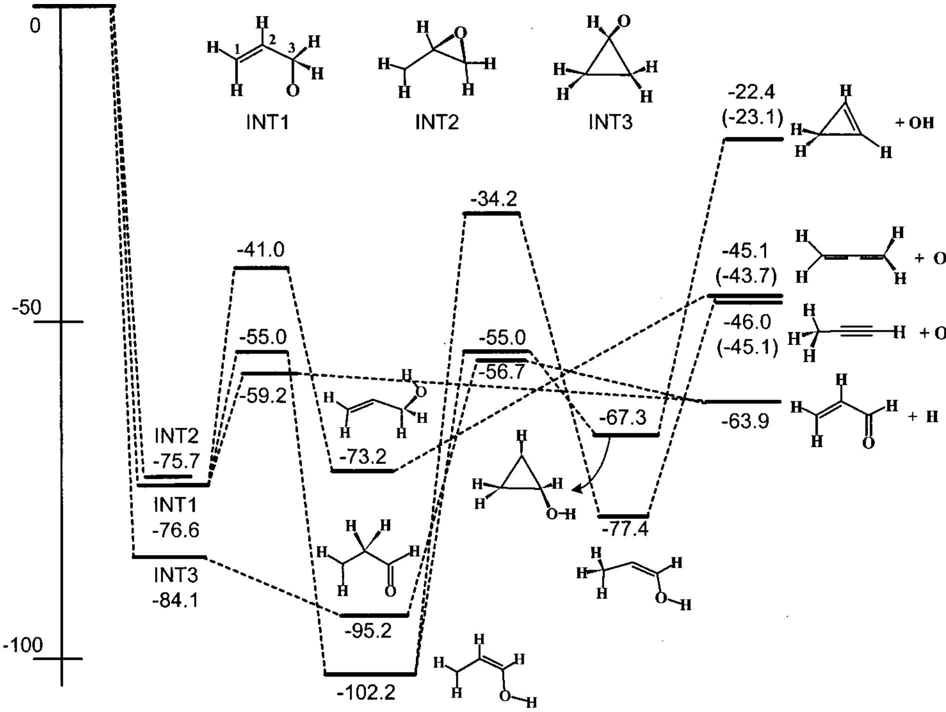

FIG. 3. Schematic energy diagram for the potential energy surface of the reaction of O(^3P) with C_3H_5 at the CBS-QB3 level of theory. The values in parentheses denote experimental values (kcal/mol).

ferences (686.0 ns for $v'=0$ and 748.4 ns for $v'=1$). The averaged partitioning ratios for the low- and high-N'' components were estimated to be 0.75 ± 0.11 and 0.50 ± 0.14, respectively, and found to be almost the same in the two spin-orbit states. The rotational populations for the F_1 and F_2 states were determined and no spin-orbit preferences were observed in either vibrational state (0.90 ± 0.16 and 1.05 ± 0.18 for $v''=0$ and $v''=1$, respectively). The Λ-doublet propensities[18] were also examined to obtain the preferential orientation of the unpaired π-orbital with respect to the plane of rotation of the diatomic product OH and the averaged ratios of $\Pi(A')/\Pi(A'')$ again represents no significant propensity (0.98 ± 0.26 and 0.93 ± 0.12 for $v''=0$ and $v''=1$, respectively).

DISCUSSION

The observed nascent internal distribution of the OH($X\,^2\Pi$) product obtained under single-collision conditions can provide detailed insights into the reactive O(^3P) $+C_3H_5$ processes and energy partitioning into products. Figure 3 shows the schematic diagram of the lowest doublet potential energy surface obtained using the CBS-QB3 level of theory. The diagram illustrates the formation of three energy-rich doublet intermediates along the entrance pathways. Addition of O(^3P) to the terminal carbon (3) forms the intermediate CH_2CHCH_2O (denoted as INT1), whereas addition to the central (2) and terminal carbons forms an O-atom bridged intermediate (INT2), lying slightly above INT1 by 0.9 kcal/mol. Another intermediate (INT3), which has more exothermicity than INT1 by 7.5 kcal/mol, is a three-membered ring of carbons. The association pathways to INT1, INT2, and INT3 are calculated to be barrierless due to the bond formation between the two radical species. In Fig. 3, the most facile reaction channel is predicted to be a direct C(3)–H bond cleavage of INT1 to form acrolein $(CH_2CHCHO)+H$. Although the barrier height is 17.4 kcal/mol, it still lies well within the available energy of the system (82 kcal/mol).[19] The exothermic acrolein pathway (1) is consistent with the observation of the previous bulk kinetic experiments.[6]

Another competing channel of INT1 involves the H-atom migration leading to C_3H_4+OH, which has been first observed in our crossed beam experiments. The counterpart of the probed OH product, C_3H_4, is known to have three different isomers: allene (CH_2CCH_2), methylacetylene (CH_3CCH), and cyclopropene. While the allene and methylacetylene channels show nearly the same exothermicities of -45.1 and -46.0 kcal/mol, respectively, the cyclopropene channel is calculated to be less exothermic (-22.4 kcal/mol). The pathway to allene involves the H-atom migration from the central carbon(2) of INT1 to the oxygen atom followed by direct decomposition to allene$+$OH. The barrier height of the migration step is calculated to be 35.6 kcal/mol, which belongs in the typically known range of $20\sim40$ kcal/mol for the H-atom migration processes. For methylacetylene and cyclopropene channels, INT1 might first undergo H-migration from the carbon(3) to the oxygen atom to form $CH_2CHCHOH$ through overcoming a low barrier of 21.6 kcal/mol. Then $CH_2CHCHOH$ might undergo either a second [1,2]-H-migration followed by direct bond rupture to methylacetylene$+$OH, or ring closure followed by direct decomposition to cyclopropene$+$OH. In comparison to the allene pathway, the methylacetylene and cyclopropene channels should overcome significantly higher barriers of 68.0 and 47.2 kcal/mol, respectively, and obviously require one additional step to yield products. For INT2 and INT3 the calculation indeed predicts fast conversion to INT1 (with its barrier height of only 3.7 kcal/mol) and to some aldehyde intermediates undergoing unfavorable high-energy processes, respectively.[20]

For the O(^3P)-allyl system, therefore, it is highly probable that the counterpart fragment C_3H_4 of the observed OH product is believed to be allene through the intermediate INT1 after taking into account the factors of reaction enthalpy, barrier height and the number of intermediates involved. It is worthwhile obtaining the energy-specific rate constants for the unimolecular decomposition pathways of the energized INT1 using the RRKM model. At our available energy of 82 kcal/mol, the rate constants for acrolein, allene, methylacetylene and cyclopropene channels are 8.1×10^{12}, 1.2×10^{10}, 1.5×10^{6}, and 2.4×10^{5} s^{-1}, respectively, which reveals the branching ratio and further supports the major acrolein+H channel and the allene+OH channel. The prediction is also quite consistent with recent theoretical calculations for the reaction of O(^3P) with halogenated alkyl radicals,[21] in which the energy-rich association intermediates similar to INT1 in our system were formed and the major decomposition product was determined by the aforementioned factors.

To better characterize the available energy partitioning into rovibrational states, the observed bimodal distributions are compared to those predicted by the *prior* statistical theory. For polyatomic systems the prior distributions are determined by the available volumes in the phase space of the two fragments, and are constrained only by energy conservation. The prior calculations predict much higher rotational temperatures (4800 K (F_1) and 4710 K (F_2) for $v''=0$, and 2920 K (F_1) and 2840 K (F_2) for $v''=1$) and a smaller fraction ($P_1/P_0=0.33$) of population partitioned into $v''=1$ compared to the observed experimental distributions. The surprisal analysis is also performed. However, the rotational surprisals for the low- and high-N'' components fit very poorly except for the large negative slope in the low-N'' regime indicating that the low rotational components are highly populated in comparison to the expected statistical distribution. The disagreement suggests that the statistical picture is not suitable to describe the reactive atom-radical processes and that the nascent internal distributions with bimodal features show clear dynamical biases.

The observed bimodal internal distributions are quite unusual in cases of reactions of ground-state atomic oxygen. The common reaction mechanism of O(^3P) with saturated hydrocarbon has been known to proceed through collinear direct abstraction pathways resulting in the vibrationally hot and rotationally cold distributions of the OH product.[22] Highly populated low-N'' components in Fig. 2 might be dominated by such direct abstraction dynamics yielding the observed high vibrational partitioning ratios and low rotational temperatures. In contrast the extraordinarily hot rotational distribution observed in this work implies that some fraction of the reactants is sampled to proceed through an addition complex such as INT1 in the potential energy surface. However, such an intermediate is not likely to be long-lived enough to allow the available energy to be statistically partitioned among all the degrees of freedom prior to dissociation, as evidently manifested in the comparison to the prior analysis. The fast and random decomposition behavior of the short-lived, energy-rich intermediate is also quite consistent with the equally populated Λ-doublet and spin-orbit components. Due to the poor fit in the statistical population analysis the relative contribution of each mechanism is not determined except for the fact that the reaction takes place mainly through a direct mechanism, rather than a complex-forming process, as clearly shown in Fig. 2. Similar bimodal distributions have rather been observed in the exothermic O(^1D)-saturated hydrocarbon reactions in which the low-N'' regime with low vibrational excitation (less than 0.1 for P_1/P_0) is well characterized by the Boltzmann-type distribution assuming the long-lived alcohol intermediate, while the high-N'' regime is described in terms of the short-lived insertion process.[23–28] Such vibrationally cold and statistical low-N'' components stand in sharp contrast to our nonstatistical low-N'' distribution with high vibrational excitation ($P_1/P_0=0.75\pm0.11$). However, the minor contribution, if any, from a long-lived complex embedded in the low-N'' regime cannot be ruled out in this work.

In summary the nascent rovibrational distributions of the OH product from the newly observed exothermic reaction of $O(^3P)+C_3H_5\rightarrow C_3H_4+OH$ were studied. To the best of our knowledge the atom-radical reaction dynamics was first probed through the combination of crossed beams and LIF techniques. The distributions showed significant bimodal internal excitations without spin-orbit and Λ-doublet propensities. With the aid of *ab initio* and statistical calculations the reactive scattering may be explained by two competing nonstatistical dynamical mechanisms: a major direct abstraction process and a minor indirect short-lived complex-forming addition process.

One of the authors (J.H.C.) wishes to thank Professor H. Reisler for her invaluable help in the development of the crossed beam apparatus, and the MOE and KBSI programs. J.H.P. and H.L. wish to acknowledge the support of BK21 fellowships. This work was financially supported by the CRM-KOSEF (2001).

[1] D. W. Kohn, H. Clauberg, and P. Chen, Rev. Sci. Instrum. **63**, 4003 (1992).

[2] I. Fischer, Chimia **54**, 96 (2000).

[3] H. J. Deyerl, I. Fischer, and P. Chen, J. Chem. Phys. **110**, 1450 (1999) and references therein.

[4] D. Stranges, M. Stemmler, X. Yang, J. D. Chesko, A. G. Suits, and Y. T. Lee, J. Chem. Phys. **109**, 5372 (1998) and references therein.

[5] M. Yamaguchi, J. Mol. Struct. THEOCHEM **365**, 143 (1996).

[6] I. R. Slagle, J. R. Bernhardt, D. Gutman, M. A. Hanning-Lee, and M. J. Pilling, J. Phys. Chem. **94**, 3652 (1990).

[7] T. Baer and W. L. Hase, *Unimolecular Reactions Dynamics* (Oxford University Press, New York, 1996).

[8] K. A. Holbrook, M. J. Pilling, and S. H. Robertson, *Unimolecular Reactions*, (Wiley, New York, 1996).

[9] H. K. Kim, H. C. Kwon, J. H. Park, Y. S. Choi, and J. H. Choi, Bull. Korean Chem. Soc. **20**, 1441 (1999); J. H. Park, H. Lee, H. C. Kwon, H. K. Kim, Y. S. Choi, and J. H. Choi (unpublished).

[10] R. Zhang, W. J. Zande, M. J. Broikowski, and R. N. Zare, J. Chem. Phys. **94**, 2704 (1991); J. Han, X. Chen, and B. R. Weiner, Chem. Phys. Lett. **332**, 243 (2000).

[11] Y. Hurwitz, P. S. Stern, R. Naaman, and A. B. McCoy, J. Chem. Phys. **106**, 2627 (1997).

[12] G. M. Sweeney, A. Watson, and K. G. Mckendrick, J. Chem. Phys. **106**, 9172 (1997).

[13] C. Lee, W. Yang, and R. G. Parr, Phys. Rev. B **37**, 785 (1988).

[14] A. D. Becke, J. Chem. Phys. **96**, 2155 (1992); **98**, 1372 (1993); **98**, 5648 (1993).

[15] L. A. Curtiss, K. Raghavachari, P. C. Redfern, and J. A. Pople, J. Chem. Phys. **106**, 1063 (1997).

[16] J. A. Montgomery, Jr., M. J. Frisch, J. W. Ochterski, and G. A. Petersson, J. Chem. Phys. **110**, 2822 (1999).

[17] M. J. Frisch, G. W. Trucks, H. B. Schlegel *et al.* GAUSSIAN 98, Revision A.7, Gaussian, Inc., Pittsburgh, PA, 1998.

[18] M. J. Bronikowsk, and R. N. Zare, Chem. Phys. Lett. **166**, 5 (1990).

[19] The available energy E_{avl} is given by the expression, $E_{\mathrm{avl}}=E_{\mathrm{com}}+E_{\mathrm{int}}(C_3H_5)-\Delta H_{rxn}$. E_{com} is the center-of-mass collision energy for the O(^3P)-allyl system, and is estimated to be 6.4 kcal/mol assuming a full expansion of the molecular beams. $E_{\mathrm{int}}(C_3H_5)$ is the internal energy of the allyl radical, and is found to be negligibly small (0.4 kcal/mol) in the supersonic molecular beam (Ref. 9) and ΔH_{rxn} is an enthalpy of formation for the intermediate of interest. The available energy for INT1 is thus estimated to be 82 kcal/mol.

[20] J. H. Park, H. Lee, Y. S. Choi, and J. H. Choi (unpublished).

[21] H. Hou, B. Wang, and Y. Gu, J. Phys. Chem. A **103**, 8075 (1999).

[22] K. Kleimermanns and A. C. Luntz, J. Chem. Phys. **77**, 3533 (1982).

[23] A. C. Luntz, J. Chem. Phys. **73**, 1143 (1980).

[24] C. R. Park and J. R. Wiesenfeld, J. Chem. Phys. **95**, 8166 (1991).

[25] Y. Rudich, Y. Hurwitz, G. J. Frost, V. Vaider, and R. Naaman, J. Chem. Phys. **99**, 4500 (1993).

[26] K. Honma, J. Chem. Phys. **99**, 7677 (1993).

[27] S. I. Wada and K. Obi, J. Phys. Chem. A **102**, 3481 (1998).

[28] M. Gonzalez, M. P. Puyuelo, J. Hernando, R. Sayos, P. A. Enriquez, J. Guallar, and I. Banos, J. Phys. Chem. A **104**, 521 (2000).